ChemComm

Accepted Manuscript

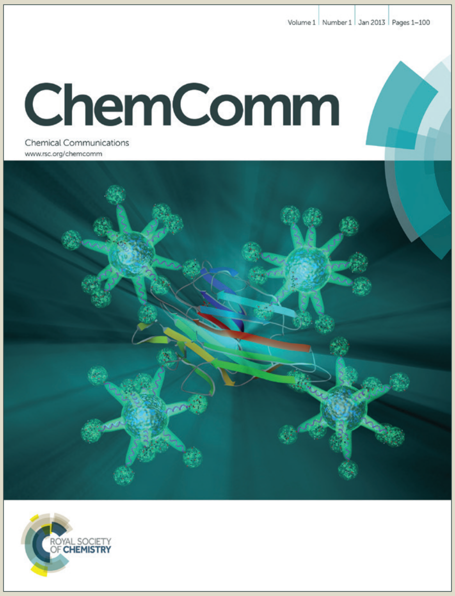

ROYAL SOCIETY OF CHEMISTRY

www.rsc.org/chemcomm

A high-performance aptasensor for mercury(II) based on the formation of unique ternary structure of aptamer-Hg^{2+}-neutral red

Cai Gao, Qingxiang Wang*, Feng Gao, Fei Gao

Received (in XXX, XXX) Xth XXXXXXXXX 200X, Accepted Xth XXXXXXXXX 2013
First published on the web Xth XXXXXXXXX 200X
DOI: 10.1039/b000000x

A highly sensitive and selective electrochemical aptasensor for mercury (II) has been developed based on the formation of a ternary complex between mercury (II) specific aptamer (MSA), neutral red (NR) molecule and Hg^{2+} ion without pre-modification of the probe aptamer.

Functional nucleic acids acted as ligand-binding agents (aptamers) attract increasing attention in biosensor construction, because they can specifically recognize various targets through tuning the base sequences.[1] To be specific, the thymine-thymine (T-T) mismatches in DNA duplexes can selectively and tightly bind with Hg^{2+}, to form thymine-Hg^{2+}-thymine (T-Hg^{2+}-T) mediated DNA duplexes.[2] Based on this feature, the T-rich oligonucleotide has been frequently applied as mercury(II) specific aptamer (MSA) for electrochemical sensing analysis of Hg^{2+}. For example, Liu *et al.*[3] have exploited an electrochemical Hg^{2+} sensor using ferrocene (Fc)-tagged MSA as the sensing element. When the MSA was interacted with Hg^{2+} and underwent conformational switch from flexible single-stranded state to the rigid duplex through T-Hg^{2+}-T coordination chemistry, the electroactive Fc tag was drawn away from the electrode surface, resulting in the decrease of the redox peaks of Fc tag. Wu *et al.*[4] have also developed a Hg^{2+} electrochemical sensor based on MSA and its Fc-tagged complementary DNA. When the Hg^{2+} was present, the MSA also underwent conformational switch from single-stranded form to the folded hairpin structure, resulting in the release of the Fc-labeled complementary strand from the electrode surface. As a result, the redox peak currents of Fc tags substantially decreased. More recently, Xuan *et al.* developed a immobilization-free and Exonuclease III-assisted amplified strategy for Hg^{2+} detection.[5] In that assay, a methylene blue (MB) modified MSA was used as the electroactive capture probe for Hg^{2+}, and then the electrochemical response of MB that released from Exonuclease III digested T-Hg^{2+}-T mediated DNA duplexes was utilized for Hg^{2+} monitoring.

However, all these sensors have one common characteristic, *i.e.*, the involved oligonucleotide including MSA or its auxiliary strands need to be pre-labeled with an electroactive signal molecule (like Fc or MB) for signal output.[3-5] This on one hand increases the preparation cost and operation time of the sensor since the biojunction process is usually sophisticated and complicated, and on the other hand the analytical sensitivity of the sensor is seriously restricted as one MSA strand can only be labeled with one signal molecule. To overcome these disadvantages, some electroactive intercalator-based aptasensors were constructed.[6-8] In these sensors, the complicated labeling procedures of the signal molecules are not needed, and meanwhile the higher sensitivity was produced through the "signal-on" mode. But because these sensors just work on the dependence of the relatively weak intercalation of the signal molecules into the target-bound aptamers, the signal stability and reproducibility are usually limited during the operation processes of rinsing and measurements. In this communication, we developed a novel and facile electrochemical Hg^{2+} aptasensor based on the formation of a stable ternary complex between MSA, neutral red (NR) and Hg^{2+}. Scheme 1 shows the construction strategy of the biosensor and the detailed working mechanism and fabrication procedures were provided in the Electronic Supplementary Materials (ESI).

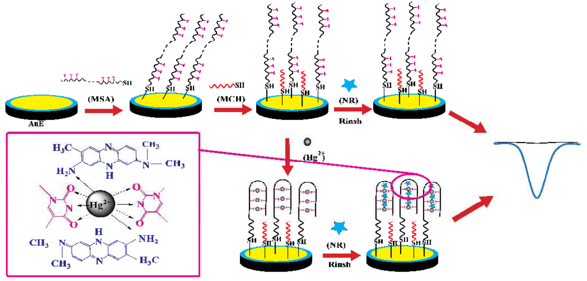

Scheme 1 Schematic representation of the preparation and working principle of the Hg^{2+} aptasensor based on the aptamer-Hg^{2+}-neutral red ternary

Fig. 1A shows the typical voltammetric characteristics of the aptasensor in response to Hg^{2+}. From the figure, it was clearly observed that not any Faradic current response was observed at Hg^{2+}/MCH-MSA/AuE (curve a), suggesting that the film of Hg^{2+}/MCH-MSA is electro-inactive under the measured conditions. However when Hg^{2+}/MCH-MSA/AuE was measured after incubating in NR solution, a pair of well-defined redox peaks was observed at -0.56 V and -0.62 V (curve c), respectively, which was in good accordance with the characteristic electrochemical response of NR.[9] This result demonstrated that the electrochemical response of the sensor is strictly depended on the presence of Hg^{2+}.

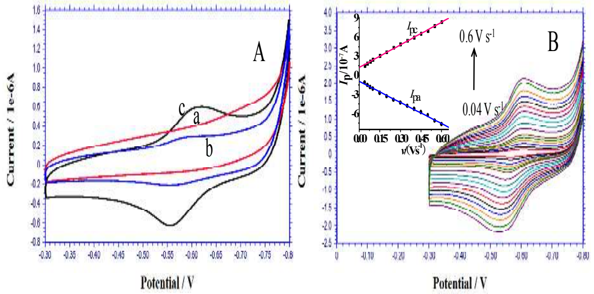

Fig.1 (A) CVs of the Hg^{2+}/MCH-MSA/AuE (a), NR/MCH-MSA/AuE (b), NR/Hg^{2+}/MCH-MSA/AuE (c) in 40 mM B-R (pH 7.0) buffer solution. (B) CVs of NR/Hg^{2+}/MCH-MSA/AuE in 40 mM B-R at different scan rates (from 0.02 V s^{-1} to 0.60 V s^{-1}). Inset shows the plots of peak currents (I_p) versus scan rate (v). The concentration of Hg^{2+} is 8.5×10^{-9} M.

The scan rate (v) experiments further showed that the redox peaks of NR enhanced regularly with the increase of the scan rate (Fig. 1B), and the redox peak currents (I_p) presented good linear relationships with v in the range from 0.02 V s^{-1} to 0.60 V s^{-1} (inset in Fig. 1 B): I_{pa} (10^{-7}A) = -0.8586-11.2745 v (V s^{-1}) and I_{pc} (10^{-7} A) = 1.1877+11.9281 v (V s^{-1}) with the correlation coefficients (r) of -0.9971 and 0.9991, respectively, which is a typical characteristic of adsorption-controlled process.[10] As a control, the electrochemical response of NR on the MCH-MSA/AuE without pre-accumulation with Hg^{2+} was also investigated, and the result revealed that only a pair of very small redox peaks was observed (curve b), which was likely caused by the weak electrostatic interaction between MSA and NR. This difference further confirmed that the electrochemical response of NR on the sensor was dependent on the presence of Hg^{2+}. Therefore, it could be concluded that NR was capable of being used as an effective electrochemical probe to monitor the Hg^{2+}.

Additionally, it could be imaged that the adsorption amount of signal probe on the sensing interface plays an important role to decide the sensitivity of the sensor. In this work, the maximum binding amount of NR on the sensor was calculated through varying NR accumulation concentration (C_{NR}). Fig. S3 in ESI shows the relationship of the coulometric charge (Q) versus the $C_{NR.}$ It could be seen that the plot had an “isotherm-like” shape. Thus according to the Langmuir model:[11] C_{NR}/Q = C_{NR}/Q_∞ +1/(KQ_∞), a saturation charge (Q_∞) of 0.3 μC with a binding constant (K) of 8.45×10^4 M^{-1} of NR on the sensor was obtained. Further, based on formula of $\Gamma_\infty=NQ_\infty/nFA$ (where N is the Avogadro's constant, A the geometric area of AuE, n the electron transferred number of NR, F Faraday constant), the saturated coverage value (Γ_{NR}) of NR was yielded to be 2.98×10^{13} molecules cm^{-2}. In addition, from the typical chronocoulometric curves of MCH-MSA/Au in Tris-HCl without (curve a) and with 50 μM $[Ru(NH_3)_6]^{3+}$ (curve b) as showed Fig. S4 in ESI, the surface density of the MSA (Γ_{MSA}) was determined to be 3.78×10^{12} molecules cm^{-2} according to the method proposed by Steel *et al.*[12] Then, the binding ratio of NR to Hg^{2+}-MSA, Γ_{NR}: Γ_{MSA}, was determined to be 7.9. This meant that each Hg^{2+}-MSA strand adsorbed eight NR molecules on average, which was significantly greater than that in the covalently modified electroactive MSA generally with the stoichiometric ratio of 1:1.[3-5] This increased absorption amount of the signal molecule is helpful to improve the sensitivity of the developed sensor.

Furthermore, the binding mechanism of NR on the sensor interface was investigated. It had been widely reported that the planar aromatic molecule of NR could intercalatively interacted with dsDNA.[9,10] Also it has been pointed out that Hg^{2+} induced hairpin-like secondary structure of MSA poses the similar characteristic and function of dsDNA.[13] Therefore, we deduced that NR should interact with Hg^{2+}-MSA adduct through intercalating into the space between the adjacent T-Hg^{2+}-T units. In order to testify this speculation, the interaction of NR with Hg^{2+}-MSA was probed through the ultraviolet (UV) spectra assays, and the results were depicted in Fig. 2A. As seen, the free MSA solution presented a characteristic absorption peak at 260 nm assigning to absorption of the bases on MSA (curve a),[14] and the free NR solution also displayed an absorption peak around 270 nm (curve b). When Hg^{2+} was added into the MSA solution, it was found that the absorption peak of MSA decreased obviously (curve c). This hypochromic effect could be explained by the formation of the duplex structure of MSA in the presence of Hg^{2+}, and the resonance of the base aromatic ring buried within duplex was limited. However when the NR was added into the system of MSA-Hg^{2+}, the absorption peak was dramatically increased (curve d), which was even larger than the sum of MSA-Hg^{2+} and NR solutions. Previous reports had pointed out that when the duplex DNA was interacted with intercalators, the DNA strands would be lengthened to accommodate the intercalated molecules, and as a result the absorption intensity of the DNA would be enhanced.[15] Therefore the hyperchromic effect observed for MSA-Hg^{2+} upon interaction with NR testified that NR bound to MSA-Hg^{2+} through the typical intercalative mode.

Furthermore, the influence of the MSA-Hg^{2+} system on the visible absorption of NR was investigated. It could be observed that NR had an intense absorption peak at 538 nm (curve a, Fig. 2B), which was consistent with the absorption wavelength of NR at previous reports.[16,17] When MSA was added into the NR solution, only a slight decrease of the peak intensity was observed (Fig. 2B, curve b), likely due to the weak electrostatic interaction of the cationic NR with the phosphate backbone of MSA.[18] It was interesting that if the mixture solution of MSA-Hg^{2+} system was added, a significant blue-shift effect accompanied by the hypochromicity was observed (Fig. 2B, curve c), which was absolutely opposite to the case observed for NR intercalating into natural dsDNA.[15] Therefore, there should be another binding mode existing between NR and MSA-Hg^{2+} besides the above-mentioned intercalation. It had been reported that the coordination action between Hg^{2+} and the functional group of chromophore could induce the decrease of π-electron density of the chromophore. As a result, the blue-shift of the characteristic peak of the chromophore could be observed.[19] So, combing the above UV and visible spectra experiments, the binding mode of NR to MSA-Hg^{2+} could be supposed as the co-existence of intercalation and coordination action.

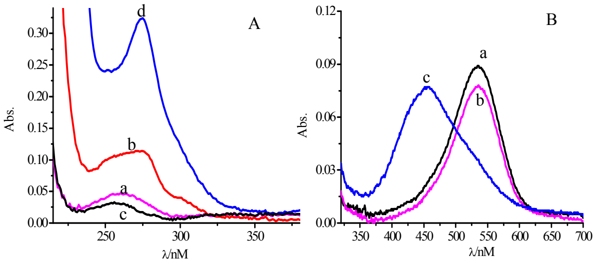

Fig. 2 (A) UV spectra of 0.1 μM MSA (a), 5.0 μM NR (b), mixture of 0.1 μM MSA and 10 μM Hg^{2+} before (c) and after interaction with 5.0 μM NR (d). (B) Visible absorption spectra of 5.0 μM NR (a), mixture of 5.0 μM NR and 0.1 μM MSA (b), and the mixture of 5.0 μM NR, 0.1 μM MSA and 10 μM Hg^{2+}(c).

Under the optimal conditions (see ESI), the DPV response of the developed aptasensor to various concentrations of Hg^{2+} was depicted in Fig. 3A. It was observed that when Hg^{2+} was absent, no obvious Faradic current signal was detected, suggesting a negligible background interference of the sensor. With the increase of Hg^{2+} concentrations ($C_{Hg}{}^{2+}$), the DPV response corresponding to NR increased accordingly, suggesting that increasing amounts of NR molecules were accumulated within the sensing layer by the formed Hg^{2+}-MSA duplex structure. The oxidation peak currents (I_{pa}) of NR presented a linear relationship with the logarithm value of $C_{Hg}{}^{2+}$ (Log $C_{Hg}{}^{2+}$) over the range from 2.7×10^{-11} M to 8.5×10^{-9} M. The linear regression equation was I_{pa} (10^{-7}A) = -1.8543Log($C_{Hg}{}^{2+}$/M) - 22.5215 with a correlation coefficient (r) of -0.9852 (Fig. 3B). Based on 3σ (σ represents the standard deviation of the blank samples, n=7), the limit of detection was estimated to be 1.5×10^{-12} M (amounting to 0.3 ppt), which was obviously lower than that of the other MSA-based electrochemical approaches (see Table S1 in ESI). Such a low detection limit was also much lower than the toxicity level of Hg^{2+} defined by the US Environmental Protection Agency (EPA) in drinkable water (<10 nM, amounting to 2 ppb),[20] suggesting that the developed approach had great promising for the sensitive monitoring of Hg^{2+} in water sample.

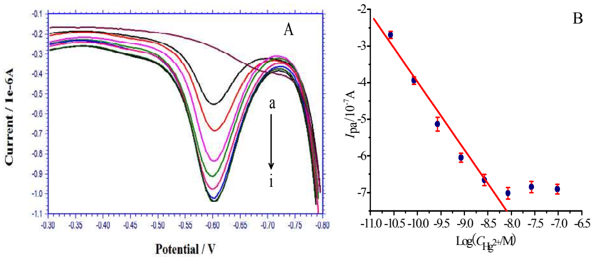

Fig. 3**.** (A) Typical DPVs of the electrochemical sensor in 40 mM B-R (pH 7.0) buffer solution in response to 0 (a), 2.7×10^{-11} M (b), 8.5×10^{-11} M (c), 2.7×10^{-10} M (d), 8.5×10^{-10} M (e), 2.7×10^{-9} M (f), 8.5×10^{-9} M (g), 2.7×10^{-8} M (h) and 8.5×10^{-8} M (i) Hg^{2+}. (B) Plot of peak currents (I_{pa}) versus the logarithm of Hg^{2+} concentrations (Log $C_{Hg^{2+}}$).

In order to probe the selectivity of the electrochemical sensor, the DPV response of the sensor to the other ions (including Ca^{2+}, Mg^{2+}, Zn^{2+}, Ni^{2+}, Ag^{+}, Cu^{2+}, Cd^{2+}, Mn^{2+}, Co^{2+}, Pb^{2+}, and K^{+}) that possibly coexisting with Hg^{2+} was investigated, and the results were summarized in Fig. S5 in ESI. As seen, the sensor showed a large DPV peak current value in response to low concentration of Hg^{2+} (8.5×10^{-9} M), but hardly exhibited substantial responses to the other metal ions even their concentrations were 100 times higher than Hg^{2+}, suggesting that the sensor possessed excellent selectivity to Hg^{2+} against other environmentally relevant metal ions. Such a high selectivity could be ascribed to specific T-Hg^{2+}-T coordination chemistry, and the unique ternary MSA-Hg^{2+}-NR structure on the sensing layer.

The Hg^{2+} sensor developed in this work could be readily regenerated by immersing the detected sensor into 1.0 mM L-cysteine (L-cys) at room temperature for 80 min and then washed with deionized water. Fig. S6 in ESI shows five runs of regeneration of this sensor. One could observe that in each run, the peak current almost recovered to the initial value after the regeneration treatment. Presumably, the formation constants (K_f≈10^{30} M^{-1})[21] of Hg-thiol complexes were significantly larger than that of T-Hg^{2+}-T base pairs (10^6 M^{-1}),[22] so the added L-cys could disrupt MSA-Hg^{2+}-NR structure by removing Hg^{2+} ions from the T-Hg^{2+}-T base pairs. The relative standard deviation (RSD) of 5.8% was estimated for five parallel measurements, indicating excellent reproducibility of the sensor.

The developed sensor was applied to detect Hg^{2+} in several real water samples that were obtained from the Jiu Longjiang River in our city and the pure drinking water and tap water in our campus. Before measurement, all the samples were filtered through a standard 0.45 µm filter. Table S2 in ESI summarized the analytical results for the five samples by our method and ICP-MS. Through comparison, it could be obtained that the relative deviation for the two methods was in the range from -5.01% to 7.71%, suggesting that the developed sensor had satisfactory reliability for the analysis of Hg^{2+} content in real samples.

In conclusion, we have developed an efficient and label-free electrochemical sensor for Hg^{2+} based on the transformation of MSA from random coil to the hairpin-like structure by Hg^{2+} and the formation of unique electroactive ternary complex of MSA-Hg^{2+}-NR. Because both the binding of MSA to Hg^{2+} and the formation of the ternary complex are specific, the sensor showed excellent selectivity and ultralow background response during testing. Compared with the conventional labeling technology-based aptasensor, the lable-free strategy developed in this communication was simpler and more labor saving. Moreover, since one Hg^{2+} bond MSA strand could associate with eight probe molecules of NR, the aptasensor could detect the target Hg^{2+} as low as 1.5 pM, which suggested that the sensor poses great promising in practical environmental monitoring.

The work is supported by the National Natural Science Foundation of China (No. 21275127), Natural Science Foundation of Fujian Province (No. 2011J01059), and Program for New Century Excellent Talents in Fujian Province University (No. JA12204)

Notes and references

[a] *College of Chemistry and Environment, Fujian Provincial Key Laboratory of Modern Analytical Science and Separation Technology, Minnan Normal University, Zhangzhou, 363000, P. R. China. Fax: +86-596-2527801; Tel: +86-596-2591445; E-mail: axiang236@126.com*

† Electronic Supplementary Information (ESI) available: [Sensing mechanism of the aptasensor, experimental details, aptasensor fabrication characterization, surface density determination of MSA, test condition optimization, and supplementary figures/tables]. See DOI: 10.1039/b000000x/

1 X. B. Yin, *TrAC, Trends Anal. Chem.*, 2012, **33**, 81–94.
2 A. Ono and H. Togashi, *Angew. Chem. Int. Ed.*, 2004, **43**, 4300–4302.
3 S. Liu, H. Nie, J. Jiang, G. Shen and R. Yu, *Anal. Chem.*, 2009, **81**, 5724–5730.
4 D. Wu, Q. Zhang, X. Chu, H. Wang, G. Shen and Yu R. *Biosens. bioelectron.*, 2010, **25**, 1025–1031.
5 F. Xuan, X. Luo and I. Hsing, *Anal. Chem.*, 2013, **85**, 4586–4593.
6 X. B. Yin, Y. Y. Xin and Y. Zhao, *Anal. Chem.*, 2009, **81**, 9299–9305.
7 F. Li, Y. Feng, C. Zhao, and B. Tang, Chem. Commun., 2011, **47**, 1909–11911
8 C. X. Tang, Y. Zhao, X. W. He and X. B. Yin, *Chem. Commun.*, 2010, **46**, 9022–9024.
9 S. Niu, S. Zhang, X. Shi and K. Jiao, *Chem. Res. Chinese U.*, 2005, **21**, 24–27.
10 H. Heli, S. Z. Bathaie and M. F. Mousavi, *Electrochem. Commun.*, 2004, **6**, 1114–1118.
11 Q. Wang, S. Li, W. Li, F. Gao and K. Jiao, *Bioelectrochemistry*, 2009, **75**, 32–36.
12 A. B. Steel, T. M. Herne and M. J. Tarlov, *Anal. Chem.*, 1998, 70, 4670–4677.
13 R. Cao, B. Zhu, J. Li and D. Xu, *Electrochem. Commun.*, 2009, **11**, 1815–1818.
14 B. Datta and G. B. Schuster, *J. Am. Chem. Soc.*, 2008, **10**, 130, 2965–2973.
15 X. Jiang, L. Shang, Z. Wang and S. Dong, *Biophys. Chem.*, 2005, **118**, 42–50.
16 G. Zhang, S. Shuang, C. Dong, D. Liu and M. M. F. Choib, *J. Photochem. Photobiol. B: Biol.*, 2004, **74**, 27, 127–134.
17 C. Z. Huang, Y. F. Li and P. Feng, *Talanta*, 2001, **55**, 321–328.
18 W. Sun, M. Yang and K. Jiao, *Int. J. Electrochem. Sci.*, 2007, **2**, 93–101.
19 M. Tian and H. Ihmels, *Chem. Commun.*,2009, 3175–3177 .
20 U.S. Environmental Protection Agency. *Edition of the Drinking Water Standards and Health Advisories*; EPA 822-S-12-001; Office of Water: Washington, DC, **2012**.
21 K. K. Divine, F. Ayala-Fierro, D. S. Barber and D. E. Carter, *J. Environ. Sci. Health, Part A*, 1999, **57**, 489 –505.
22 H. Torigoe, A. Ono and T. Kozasa, Chem. Eur. J., 2010, 16,

13218–13225.